

Electromagnetic ghosts in pair plasmas

Maxim Lyutikov

Department of Physics and Astronomy, Purdue University,
525 Northwestern Avenue, West Lafayette, IN 47907-2036

Collisions of two weakly nonlinear, $a_0 \ll 1$, counter-propagating EM pulses in pair plasma leave behind a long-surviving collection of localized waves, *an electromagnetic ghost*. Waves are trapped (localized) by the random large density fluctuations created by the beat between the pulses. The process is similar to random plasma density grating and/or Anderson-like wave localization. Structures survive for long, mesoscale times, while the EM energy slowly bleeds through high density walls of the density trap. Large guide magnetic field, $\omega_B \geq \text{few } \omega$, suppresses the formation of the ghosts.

I. INTRODUCTION

The present work touches on a number of issues in the physics of high intensity lasers, and plasma astrophysics. Modern powerful lasers can accelerate particles to relativistic velocities, resulting in the production of e^\pm pairs [1–4]. The physics of ultra-strong laser-matter interaction also became a forefront research topic in relativistic plasma astrophysics, initiated by the meteoritic developments over the last years in the field of mysterious Fast Radio Bursts (FRBs) - ultra-intense millisecond-long radio bursts coming halfway across the visible Universe [5–9]. Finally, nonlinear interaction of EM beams creates plasma density grating that is used in laser pulse compressor schemes [10, 11].

The present work follows on [12, 13] in investigating nonlinear effects in pair plasma. The key point is that in pair plasmas the density grating resulting from the nonlinear wave interactions produces charge-neutral density structures. Since there is no Coulomb repulsion, the resulting density fluctuations turn out to be much larger than in the electron-ion plasmas.

In this work we first demonstrate that interaction of weakly nonlinear waves can produce long-lived density structures in pair plasma - electromagnetic ghosts. Their dynamics occurs on mesoscales - intermediate between small kinetic and macroscopic scales. After investigating the properties of the electromagnetic ghosts, we then argue that a pair plasma subject to mildly intense electromagnetic waves becomes “granular” - a highly density inhomogeneous medium.

II. ELECTROMAGNETIC GHOSTS IN 1D

A. The code and parameters

The simulations were performed using the EPOCH code [14]. Both boundary conditions are “simple laser” (for the EM fields coming from the inside of the plasma, this is equivalent to “open” boundary condition).

Our parameters are: both lasers’ wavelengths $\lambda = 10^{-4}$ cm; plasma density $n/n_{cr} = \omega^2/\omega_p^2 = 10^{-2}$ (ω_p is defined with respect to each component separately);

slab thickness is 100λ . Laser intensity is parametrized by parameter a_0

$$a_0 = \frac{eE_w}{m_e c \omega} = 10^{-2} \quad (1)$$

The particular choice of a_0 is bounded by two factors: wave localization (formation of ghosts) increases with a_0 , yet for larger a_0 , the pair plasma is swept by the EM pulse (e.g., for as little as $a_0 = 0.03$ the density increase is of the order of unity [13]).

The strongest effect is when both pulses are circularly polarized (CP), and in the PLUS configuration, with the same sense of rotation in absolute space (not with respect to there wave vector, see [13].) In the opposite case, MINUS configuration, there is no ghosting.

A nonlinear pulse is expected to be self-localized on scales [13]

$$L \approx \frac{1}{\rho_L} \frac{c}{\omega} \\ \rho_L = \left(a_0 \frac{\omega_p}{\omega} \right)^{2/3} \approx 100, \quad (2)$$

(numerical estimate is for the parameters of these simulations), see Appendix A. Since we are interested in the effects arising due to interaction of the beams, we limit the pulse width to $\leq L$.

For 1D runs, the code parameters are set to $n_x = 100$ (number of cells per wavelength) and $n_p = 100$ (number of particles per cell). Unless specified, the initial configuration is cold plasma, see §II C 2 for discussion of thermal effects.

B. The electromagnetic ghost: basic 1D results (cold plasma, no magnetic field)

We first discuss in details the properties of the 1D simulations, and later, in §7 we explore the 2D beams, modulated in transverse and longitudinal directions

Our main result is featured in Fig. 1. We plot snapshots of Poynting flux (top row, normalized to peak value of the pulses), plasma density (middle row, normalized to

the undisturbed value) and plasma electromagnetic energy density (bottom row, also normalized to peak value of the pulses). Two CP with PLUS relative polarization.

Before the collision (top panel), the CP pulses do not disturb plasma much. During the interaction, the beat between the laser pulses produces large, random density fluctuations that survive for times much longer than the interaction time (central panel). Resulting random density fluctuations create random plasma density grating, and corresponding random fluctuations of the dielectric prematurity ϵ . These random fluctuations of ϵ Anderson-localize the electromagnetic energy (bottom panel), creating the electromagnetic ghost. The ghost survives for times much longer than the interaction time, and actually, it survives for mesoscopic time scales, much longer since the electromagnetic pulses left the simulation domain (bottom panel).

The electromagnetic energy is “sloshing” within the ghost, eventually creating well-structured density wall. The amplitude of density perturbations first even increases with time (compare middle and right panel in the middle row). The energy is slowly leaking from the ghost, as indicated by two arrows in the top right panel (one can check that the average value of Poynting flux is negative in the left half of the simulation box and positive in the right half). Drainage is not continuous, but time dependent/oscillatory, as indicated by wave-like structures of the Poynting flux outside the ghost. While at late times the density and energy density evolve slowly, the Poynting flux shows sloshing waves within the ghost, penetrating the density barrier, and propagating outwards.

The size of the ghost is approximately two times the size of each pulse - this is the interaction length of the pulses.

Since the energy density in the ghost is $\sim 10^{-4}$ of the peak energy density of the main pulses, relatively long simulations are needed to see the ghost, the main pulses need leave the box way before the ghost shows up.

In Fig. 2 we show long-term evolution of the ghost. The ghost slowly expands, remaining as a coherent structure for a very long time.

C. Guide magnetic field, plasma temperature, polarization effects

1. Effects of guide magnetic field

It is convenient to introduce parameter

$$b_0 = \frac{\omega_B}{\omega} \quad (3)$$

$b_0 = 1$ corresponds to cyclotron resonance (and efficient absorption of the wave).

Outside of the regime $b_0 \approx 1$, the effects of the guide magnetic field are as follows. For $b_0 \leq 1$ (sub-resonant pulse), the strength of the ghost do not depend much on the values of the guide field b_0 . For $b_0 \geq 1$, the strength

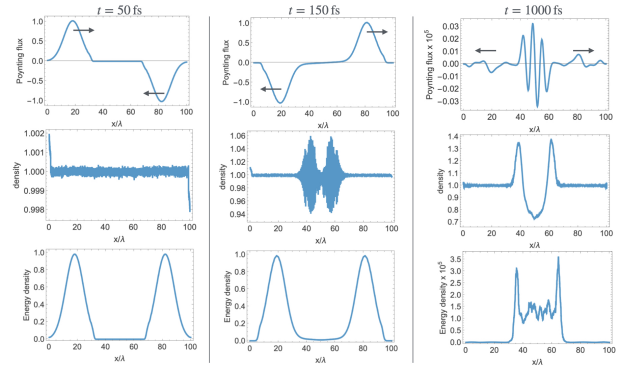


FIG. 1. Colliding EM pulses in pair plasma. Columns (left to right): snapshots at time 50 fs (before collision), 150 fs (soon after collision), 1000 fs (long after collision). Rows (top to bottom): Poynting flux, density, energy density. Poynting flux and energy density are normalized to peak values, except in the right column where they are multiplied by 10^5 . All plotted quantities are averaged over one wavelength. Peak nonlinearity $a_0 = 10^{-2}$, pulses' duration full width at half max is 50 fs. $n_x = 100$, $n_p = 100$. (Results for $n_x = 30$, $n_p = 30$ look qualitatively similar.)

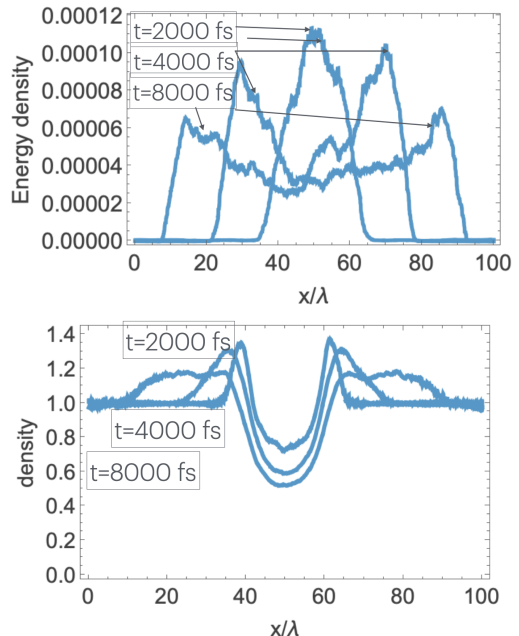


FIG. 2. Evolution of the structure of the ghost with time: profiles of energy density (top panel) and plasma density (bottom panel). With time the ghost becomes wider. With time the central density depletion increases. In these simulations $n_x = n_p = 100$.

of the ghost sharply decreases for $b_0 \geq 2$. For $b_0 = 4$ the ghost nearly disappears.

We also comment that generally one cannot compare the properties of the ghost as a function of b_0 at fixed simulation time since the EM propagation speeds, interaction time and length, all depend on magnetic field.

For $b_0 \geq 1$, the strength of the ghost decreases with b_0 .

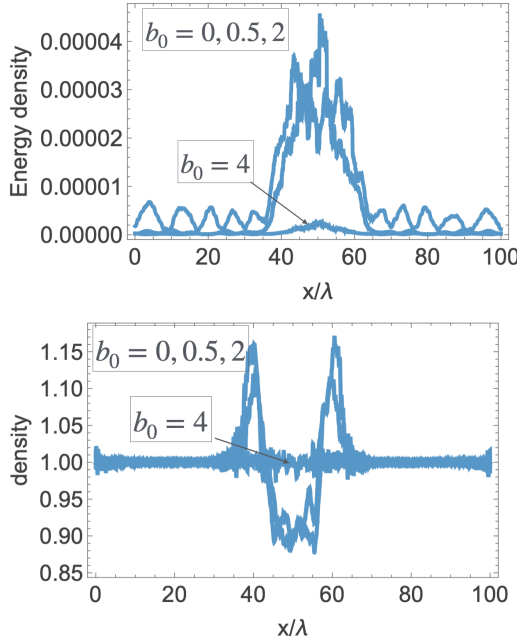


FIG. 3. Dependence of the ghost on guide magnetic field. For $b_0 = 0, 0.5, 2$ the curves are almost coincident. For $b_0 = 4$ the ghost nearly disappears. In these simulations $n_x = n_p = 100$.

2. Initial temperature

For initially hot plasma, the physically relevant parameter is

$$\Theta_0 \equiv \frac{k_B T}{m_e c^2} = a_0^2 \quad (4)$$

For $\Theta > \Theta_0$ the thermal velocity of particles exceeds the jitter velocity in the wave. This leads to decoherence, and ghosts disappear. Our numerical results are in agreement with this prediction. In Fig. 4 we plot profiles of energy density for one particular value of $\Theta = 0.5 \times a_0^2 = 5 \times 10^{-5}$. The ghost is nearly gone.

Investigation of a particular dependence on temperature (at smaller Θ) requires heavy calculations. Due to numerical heating, initially cold plasma achieves condition $\lambda/n_x \approx 10r_D$ [r_D is Debye radius, 15]. The corresponding numerical temperature is

$$\Theta_{num} \approx \frac{1}{n_x^2} \left(\frac{n}{n_{cr}} \right) \quad (5)$$

Condition $\Theta_{num} \leq \Theta_0$ then requires resolution:

$$n_x \geq \frac{1}{a_0} \left(\frac{n}{n_{cr}} \right)^{1/2} \approx 10 \quad (6)$$

Our numerical results conform with this estimate.

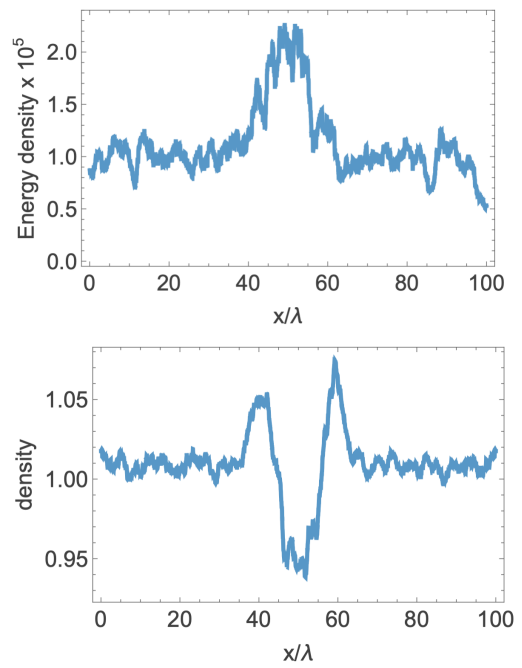


FIG. 4. Effect of temperature. At $\Theta = 0.5 \times a_0^2 = 5 \times 10^{-5}$ the ghost is nearly gone (and even weaker for larger temperatures).

3. Density granulation

Density perturbations induced by weakly nonlinear electromagnetic waves survive in pair plasma for a very long time. As a result, pair plasma subjected to a burst of electromagnetic waves becomes “granular”, with large density fluctuations, even long after the pulses exited the plasma. In Fig. 5 we show density structure after 5 pulses from each side passed through (10 pulses total). Each pulse has a duration of 50 fs, pulses are separated by 100 fs. The last pulse left the simulation domain around 500 fs - snapshot is taken at 4000 fs.

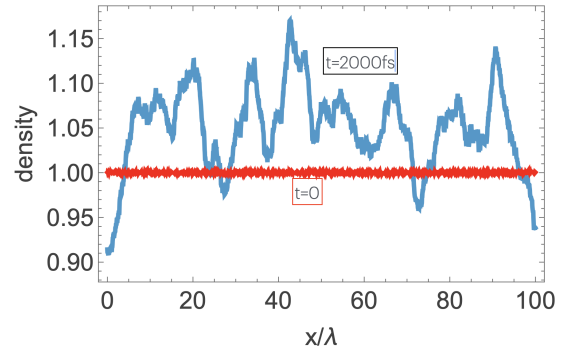


FIG. 5. Density structure after collision of 5+5 pulses, at time $t = 4000$ fs, compared with the undisturbed plasma. Density is averaged over one wavelength. Slight overall increase is due to ponderomotive push from the pulses.

III. ELECTROMAGNETIC GHOSTS IN 2D

We have run a number of 2D simulations. The transverse Gaussian profile was set to 5λ , Figs. 6- 7. The 2D simulations are generally consistent with the 1D simulations: an electromagnetic cavity is formed. These 2D simulations importantly demonstrate that the 1D simulations/results are generic, not specifically limited to low dimensionality.

In Fig. 6 we depict the basic case, the formation of the electromagnetic ghost following an encounter of two electromagnetic pulses in unmagnetized plasma. A low density/high electromagnetic density 2D cavity is formed. Both the transverse and longitudinal extents match the expectation.

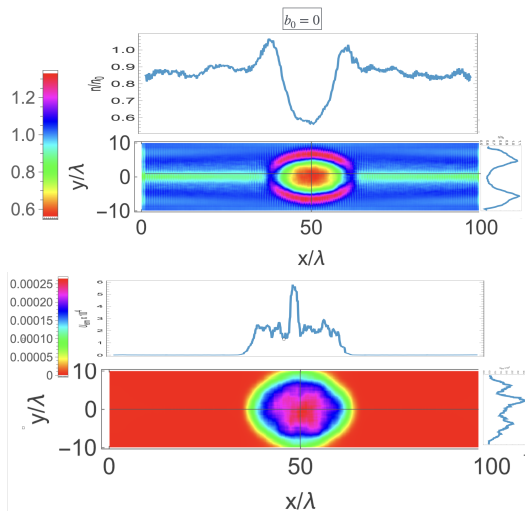


FIG. 6. 2D simulations of electromagnetic ghost, zero guide fields. Density (top) and electromagnetic energy density (bottom), time 1000 fs; attached panels are middle cuts. Energy density is normalized to the peak energy density of the pulses; typical value within the ghost is 10^{-4} ($n_x = n_p = 30$).

Magnetized 2D cases, Fig. 7, also follow the 1D simulations: cavities are formed for $b_0 \leq \text{few}$. For sufficiently high guide magnetic field ghosts also disappear in 2D.

IV. DISCUSSION

We discovered a new nonlinear plasma effect: electromagnetic ghosts created by colliding pulses in pair plasma. The effect we are after is different from electrostatic echos/van Kampen waves [16, 17]. In our case,

the trapped waves are electromagnetic.

There are several stages to trapping. At first, density fluctuations are random, appearing on scales of wavelength, and extend over the interaction length, approximately two times the size of the wave-packet. This is the regime of Anderson localization [18], or, more correctly, localization of light in random media [19, 20]. One may classify this as a linear trapping regime.

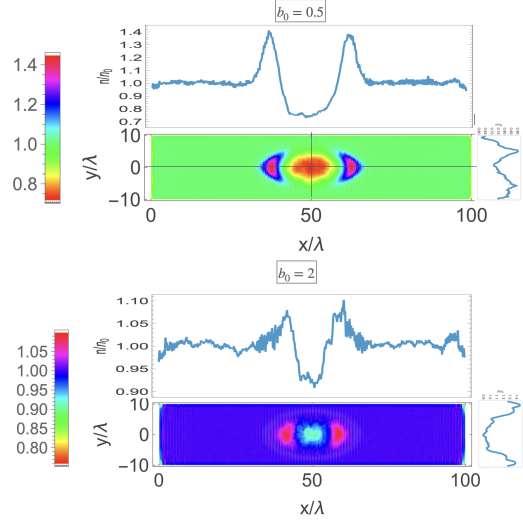


FIG. 7. 2D simulations with guide magnetic field field. Depicted are plasma density structures for $b_0 = 0.5, 2$, Top and right panels are middle cuts.

As the original wave-packets leave, the electromagnetic energy trapped inside the ghosts effectively pushes on the confining structures, sweeping plasma and leading to the generation of homogeneous density walls. One may classify this as a nonlinear trapping regime. With time, the trapped electromagnetic fields push the confining walls outwards. This, on the one hand, decreases the internal energy density of radiation, and, curiously, deepens the density well, bottom panel in Fig. 2.

These effects persist for not too strong magnetic fields, $\omega_B \leq \text{few } \omega$.

We have also considered linear polarization (LP). For aligned case, when the polarization planes coincide, the ghost is also present, similar to the CP case. Each LP pulse can be approximated by two CP pulses, forming two pairs of PLUS configurations. For orthogonal LPs there is no ghost.

This research was supported in part by grant NSF PHY-2309135 to the Kavli Institute for Theoretical Physics (KITP). I would like to thank Paulo Alves, Goetz Lehmann, Alexey Mohov, Alexander Philippov, Anatoly Spitkovsky and Kavin Tangtarharakul.

[1] M. Marklund and P. K. Shukla, *Reviews of Modern Physics* **78**, 591 (2006), hep-ph/0602123.

[2] A. R. Bell and J. G. Kirk, *Phys. Rev. Lett.* **101**, 200403 (2008), 0808.2107.

[3] C. P. Ridgers, C. S. Brady, R. Duclous, J. G. Kirk, K. Bennett, T. D. Arber, A. P. L. Robinson, and A. R. Bell, Phys. Rev. Lett. **108**, 165006 (2012), 1202.2848.

[4] P. Zhang, S. S. Bulanov, D. Seipt, A. V. Arefiev, and A. G. R. Thomas, Physics of Plasmas **27**, 050601 (2020), 2001.00957.

[5] D. R. Lorimer, M. Bailes, M. A. McLaughlin, D. J. Narkevic, and F. Crawford, Science **318**, 777 (2007), 0709.4301.

[6] M. Lyutikov, L. Burzawa, and S. B. Popov, MNRAS **462**, 941 (2016), 1603.02891.

[7] E. Petroff, J. W. T. Hessels, and D. R. Lorimer, Astron. Astrophys. Rev. **30**, 2 (2022), 2107.10113.

[8] J. M. Cordes and S. Chatterjee, ARAA **57**, 417 (2019), 1906.05878.

[9] L. G. Spitler, P. Scholz, J. W. T. Hessels, S. Bogdanov, A. Brazier, F. Camilo, S. Chatterjee, J. M. Cordes, F. Crawford, J. Deneva, et al., Nature (London) **531**, 202 (2016), 1603.00581.

[10] M. R. Edwards and P. Michel, Physical Review Applied **18**, 024026 (2022).

[11] G. Lehmann and K. H. Spatschek, Phys. Rev. E **110**, 015209 (2024).

[12] K. Tangtarharakul, A. Arefiev, and M. Lyutikov, arXiv e-prints arXiv:2509.06230 (2025), 2509.06230.

[13] M. Lyutikov and V. Gurarie, arXiv e-prints arXiv:2509.20594 (2025), 2509.20594.

[14] T. D. Arber, K. Bennett, C. S. Brady, A. Lawrence-Douglas, M. G. Ramsay, N. J. Sircombe, P. Gillies, R. G. Evans, H. Schmitz, A. R. Bell, et al., Plasma Physics and Controlled Fusion **57**, 1 (2015).

[15] C. K. Birdsall and A. B. Langdon, *Plasma Physics via Computer Simulation* (1991).

[16] B. B. Kadomtsev, Soviet Physics Uspekhi **11**, 328 (1968), URL <https://doi.org/10.1070/PU1968v01n03ABEH003837>.

[17] N. G. Van Kampen, Physica **21**, 949 (1955).

[18] P. W. Anderson, Physical Review **109**, 1492 (1958).

[19] M. E. Gertsenshtein and V. B. Vasiliev, Theory of Probability & Its Applications **4**, 391 (1959).

[20] S. John, Physics Today **44**, 32 (1991).

[21] R. M. Cherian, N. Varghese, and R. S. Sooraj, Plasma **5**, 499 (2022).

[22] P. Alves, R. Trines, K. Humphrey, R. Bingham, A. Cairns, F. Fiúza, R. Fonseca, L. Silva, and P. Norreys, arXiv e-prints arXiv:1311.2034 (2013), 1311.2034.

Appendix A: Anderson self-localization of long pulses

In pair plasma, long EM pulses experience Anderson self-localization. One of the consequences is that a sufficiently long pulse, exceeding (2) is reflected from plasma [13], Fig. 8.

This has implications for schemes based on laser amplification via stimulated Brillouin scattering [21, 22], that use two counter-propagating laser pulses. The length of the pump is usually a free parameter. In pair plasma it is not: it is limited by Anderson self-localization of the pump pulse [13]. After traversing the length (2) the pump self-localizes/reflects: in pair plasma the effective pump duration is limited by (2). This limitation on Stimulated Brillouin back-scattering is specific to pair plasma.

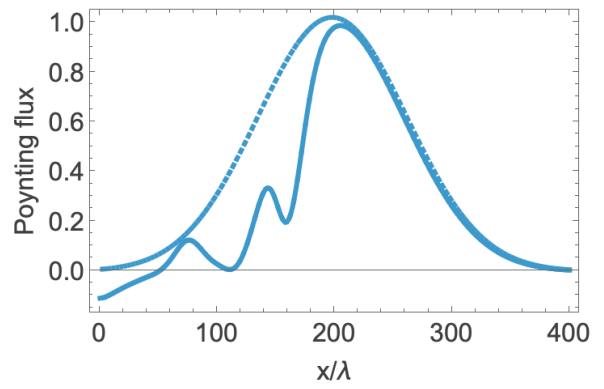


FIG. 8. Self-localization of the pump. Plotted are Poynting fluxes, normalized to peak value, pulse duration 1000 fs. Dashed line is vacuum profiles, solid line: pair plasma. The pump pulse in plasma is cut-off, approximately after ρ_L , Eq. (2). This is due to Anderson self-localization of the pump [13]. Notice negative values of Poynting fluxes at small x , indicating that energy is been drained from the pulse.